available at www.sciencedirect.com

ScienceDirect

www.elsevier.com/locate/brainres

BRAIN RESEARCH

Research Report

Effects of heat stress on Young's modulus of outer hair cells in mice

Michio Murakoshi[a,1], *Naohiro Yoshida*[b,1], *Yoko Kitsunai*[a], *Koji Iida*[a], *Shun Kumano*[a], *Takashi Suzuki*[a], *Toshimitsu Kobayashi*[b], *Hiroshi Wada*[a,*]

[a]*Department of Bioengineering and Robotics, Tohoku University, 6-6-01 Aoba-yama, Sendai 980-8579, Japan*
[b]*Department of Otolaryngology, Tohoku University, Graduate School of Medicine, 1-1 Seiryo-machi, Sendai 980-8574, Japan*

ARTICLE INFO

Article history:
Accepted 30 May 2006
Available online 5 July 2006

Keywords:
Heat stress
Outer hair cell
Young's modulus
Filamentous actin
Atomic force microscopy
Distortion product otoacoustic emission

Abbreviations:
ACh, acetylcholine
AFM, atomic force microscopy
BM, basilar membrane
CAP, compound action potential
CLSM, confocal laser scanning microscopy
DG, displacement generator
DPOAE, distortion product otoacoustic emission
F-actin, filamentous actin
FFT, fast Fourier transformation
HSP, heat shock protein
OHC, outer hair cell
PTS, permanent threshold shift
RL, reticular lamina

ABSTRACT

Intense sound exposure causes permanent hearing loss due to hair cell and cochlear damage. Prior conditioning with sublethal stressors, such as nontraumatic sound, heat stress and restraint protects the ear from acoustic injury. However, the mechanisms underlying conditioning-related cochlear protection remain unknown. In this paper, Young's modulus and the amount of filamentous actin (F-actin) of outer hair cells (OHCs) with/without heat stress were investigated by atomic force microscopy and confocal laser scanning microscopy, respectively. Conditioning with heat stress resulted in a statistically significant increase in Young's modulus of OHCs at 3–6 h after application, and such modulus then began to decrease by 12 h and returned to pre-conditioning level at 48 h after heat stress. The amount of F-actin began to increase by 3 h after heat stress and peaked at 12 h. It then began to decrease by 24 h and returned to the pre-conditioning level by 48–96 h after heat stress. These time courses are consistent with a previous report in which heat stress was shown to suppress permanent threshold shift (PTS). In addition, distortion product otoacoustic emissions (DPOAEs) were confirmed to be enhanced by heat stress. These results suggest that conditioning with heat stress structurally modifies OHCs so that they become stiffer due to an increase in the amount of F-actin. As a consequence, OHCs possibly experience less strain when they are exposed to loud noise, resulting in protection of mammalian hearing from traumatic noise exposure.

* *Corresponding author*. Fax: +81 22 795 6939.
E-mail address: wada@cc.mech.tohoku.ac.jp (H. Wada).
[1] These authors contributed equally to this work.

0006-8993/$ – see front matter © 2006 Elsevier B.V. All rights reserved.
doi:10.1016/j.brainres.2006.05.095

1. Introduction

Outer hair cells (OHCs) of the mammalian cochlea are sensory cells which have a unique capability to alter their cell length in response to changes in membrane potential (Ashmore, 1987; Brownell et al., 1985; Kachar et al., 1986; Santos-Sacchi and Dilger, 1988). Due to this so-called electromotility, OHCs subject the basilar membrane (BM) to force, thereby leading to amplification of the BM vibration. This cochlear amplification is responsible for the high sensitivity, broad dynamic range, sharp frequency selectivity and nonlinear characteristics of mammalian hearing. Unfortunately, however, OHCs, especially the first row, are vulnerable to acoustic overstimulation. Histological findings have shown that in cases with a 40-dB permanent threshold shift (PTS) after overexposure to traumatic sound, the stereocilia of OHCs are damaged without any structural damage to the supporting cells and inner hair cells (Liberman, 1987; Liberman and Dodds, 1984). The loss of OHCs causes a hearing loss of approximately 40 dB as a result of damage to the cochlear amplifier (Miller, 1974).

The susceptibility of the auditory system to hearing loss from acoustic overstimulation has been shown to decrease with repeated exposures to nontraumatic sound, a phenomenon known as "conditioning" (Miller et al., 1963). This sound induced conditioning effect has been studied in a variety of animals, including guinea pigs (Canlon et al., 1988; Kujawa and Liberman, 1997; Skellett et al., 1998), rabbits (Franklin et al., 1991), rats (Pukkila et al., 1997), chinchillas (Campo et al., 1991), gerbils (Ryan et al., 1994), mice (Yoshida and Liberman, 2000) and humans (Miyakita et al., 1992). Besides nontraumatic sound exposure, it has also been elucidated that hearing loss caused by traumatic exposure can be decreased by previous conditioning with sublethal stress, such as heat stress and physical restraint (Wang and Liberman, 2002; Yoshida et al., 1999). However, study of the effects of such conditioning on the structure and/or function of the cochlear cells has been limited. Regarding the cochlear function, it has conventionally been evaluated by measuring compound action potential (CAP) or distortion product otoacoustic emission (DPOAE). Sound and restraint but not heat stress conditioning have been found to slightly enhance the CAP threshold and CAP input–output (I–O) function without statistical significance, and DPOAEs have also been found to be slightly enhanced in conditioned ears (Kujawa and Liberman, 1999; Wang and Liberman, 2002; Yoshida and Liberman, 2000; Yoshida et al., 1999). Morphologically, it has been shown that the vesicles in the basal pole of the OHC increased after sound conditioning (Canlon et al., 1993). Filamentous actin (F-actin) in OHCs, which is a primary component of their structural filaments, has been reported to increase as a result of sound exposure, while it decreased when exposure time and/or sound pressure were changed (Hu and Henderson, 1997). Another study reported that F-actin at the bent stereocilia of OHCs decreased by exposure to high-level noise (Avinash et al., 1993).

Although these physiological and morphological studies suggest that OHCs are indeed structurally and/or functionally modified by conditioning with sublethal stress, the mechanisms underlying such structural and functional changes in OHCs and consequential conditioning-related cochlear protection remain unknown. To determine the effects of conditioning on the structure and function of OHCs in mice and to explore possible mechanisms of conditioning-related cochlear protection, Young's modulus, which indicates the elasticity of materials and is a factor determining stiffness, and the amount of F-actin, which is a primary component of cell structure, of OHCs were measured before and after conditioning by atomic force microscopy (AFM) and confocal laser scanning microscopy (CLSM), respectively. In addition, DPOAEs, which substantially rely on the electromotility of OHCs, were measured before and after conditioning. The conditioning was performed by subjecting animals to a high temperature (46.5 °C) for 15 min, i.e., heat stress, which has been proposed to be the most suitable model for exploring the mechanism of the conditioning effect on OHCs since heat stress dramatically suppresses PTS by about 25 dB in mice (Yoshida et al., 1999).

2. Results

2.1. *Changes in Young's modulus of OHCs*

The relationship between Young's modulus of the mouse OHCs in the apical turn and the cell length in each experimental group is shown in Fig. 1A. Open circles show results for the control group (n = 10), while filled circles, open diamonds, crosses, open squares and filled squares show those obtained for the anesthesia + heat groups with intervals of 3 h (n = 13), 6 h (n = 5), 12 h (n = 8), 24 h (n = 7) and 48 h (n = 12), respectively. Lengths of the apical-turn OHCs ranged from 15.5 μm to 23.0 μm and their Young's moduli ranged from 1.2 to 3.9 kPa. The regression line of the control group is given by $y = -0.025x + 2.5$ ($r = -0.11$), while those of the anesthesia + heat groups with intervals of 3 h, 6 h, 12 h, 24 h and 48 h are given by $y = -0.11\times + 4.9$ ($r = -0.23$), $y = 0.35x - 3.7$ ($r = 0.74$), $y = 0.069x + 1.3$ ($r = 0.061$), $y = 0.27x - 3.2$ ($r = 0.66$) and $y = -0.0088x + 2.6$ ($r = -0.026$), respectively. Statistical analysis indicated that there was no significant correlation between Young's modulus and the length of the OHC in the apical turn of the cochlea in each experimental group ($P > 0.05$ by Student's t-test). Young's moduli of OHCs in the anesthesia + heat groups with 3-h, 6-h and 12-h intervals tended to be larger than those of the control group and the anesthesia + heat groups with 24-h and 48-h intervals. As shown in Fig. 1B, the mean and standard deviation of Young's moduli of the apical-turn OHCs in the control group was 2.1 ± 0.5 kPa, while those in the anesthesia + heat groups with intervals of 3 h, 6 h, 12 h, 24 h and 48 h were 2.8 ± 0.8 kPa, 2.9 ± 0.6 kPa, 2.7 ± 1.0 kPa, 2.0 ± 0.3 kPa and 2.4 ± 0.6 kPa, respectively. Young's modulus of the mouse OHCs increased 1.3-fold by 3 h after heat stress and reached a peak at 6 h, which was 1.4 times as large as control level. It then began to decrease at 12 h after such stress, at which point it was still greater than that of the control group. Young's modulus returned to the pre-conditioning level by 24–48 h. Statistical analysis indicated significant differences between the control group and the anesthesia + heat groups with the two shortest intervals, i.e., 3-h and 6-h intervals, as shown by asterisks ($P < 0.05$ by Student's t-test).

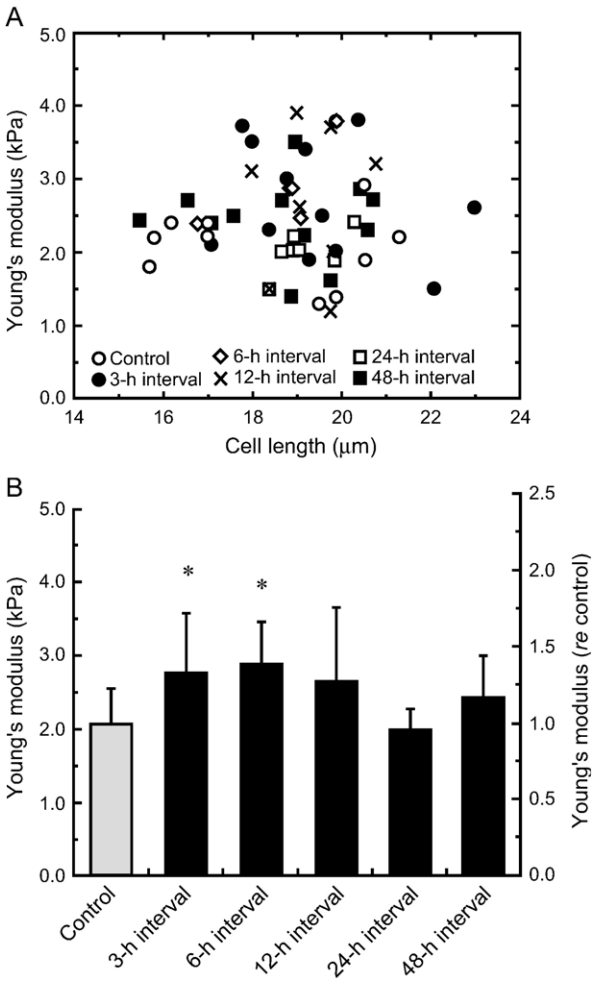

Fig. 1 – Young's modulus of the apical-turn mouse OHCs in the control group (n = 10) and the anesthesia + heat groups with 3-h (n = 13), 6-h (n = 5), 12-h (n = 8), 24-h (n = 7) and 48-h (n = 12) intervals. (A) The relationship between Young's modulus and the cell length in each experimental group. The regression line of the control group is given by $y = -0.025x + 2.5$ ($r = -0.11$), while those of the anesthesia + heat groups with intervals of 3 h, 6 h, 12 h, 24 h and 48 h are given by $y = -0.11x + 4.9$ ($r = -0.23$), $y = 0.35x - 3.7$ ($r = 0.74$), $y = 0.069x + 1.3$ ($r = 0.061$), $y = 0.27x - 3.2$ ($r = 0.66$) and $y = -0.0088x + 2.6$ ($r = -0.026$), respectively. In each experimental group, OHCs in the apical turn of the mouse cochlea statistically showed no significant correlation between Young's modulus and the cell length ($P > 0.05$ by Student's t-test). Young's moduli of OHCs in the anesthesia + heat groups with 3-h, 6-h and 12-h intervals tended to be larger than those of the control group and the anesthesia + heat groups with 24-h and 48-h intervals. (B) The mean and standard deviation of Young's moduli of the apical-turn OHCs in each experimental group. Young's modulus of the mouse OHCs increased 1.3-fold and 1.4-fold by 3 h and 6 h after heat stress, respectively, at which time it reached a peak. It then began to decrease 12 h after such stress and returned to the pre-conditioning level by 24–48 h. Statistical analysis indicated significant differences between the control group and the anesthesia + heat groups with 3-h and 6-h intervals, as shown by asterisks ($P < 0.05$ by Student's t-test).

2.2. *Changes in the amount of F-actin of OHCs*

Fig. 2A shows a fluorescence image of F-actin labeling at the lateral wall of the OHC. Fig. 2B shows the normalized average intensities of F-actin labeling of OHCs in each experimental group. Such intensities were obtained for the control group (n = 13) and the anesthesia + heat groups with 3-h (n = 10), 6-h (n = 8), 12-h (n = 6), 24-h (n = 10), 48-h (n = 10) and 96-h (n = 8) intervals. Most data for the control group and the anesthesia + heat groups showed similar intensities; however, OHCs of a cochlea in the anesthesia + heat group with a 24-h interval showed an extraordinarily high average intensity (open circle, 30.8%). This datum was statistically an outlier ($P < 0.05$ by Grubbs' test). This outlier was therefore excluded from the data set when it was subjected to further analysis. Fig. 2C shows the mean and standard deviation of the normalized average intensities of F-actin labeling in each group. The average intensity of F-actin labeling increased 1.2-fold and 1.3-fold by 3 h and 6 h after heat stress, respectively. It peaked at 12 h after such stress, at which point it was 1.5 times larger than that of the control, and began to decrease by 24 h. It then returned to the pre-conditioning level by 48–96 h. Statistical analysis indicated significant differences between the control group and the anesthesia + heat groups with intervals of 3 h, 6 h, 12 h and 24 h, as shown by asterisks ($P < 0.05$ by Student's t-test).

2.3. *DPOAE enhancement after heat stress*

DPOAEs at $2f_1$–f_2 were measured at three frequencies (f_2 = 7.4, 9.8 and 14.1 kHz) via amplitude vs. level functions before (n = 3) and 3 h after heat stress (n = 5), as shown in Fig. 3. In the present study, DPOAEs were exclusively measured 3 h after heat stress since the sequential anesthesia weakened the animals and resulted in a reduction of DPOAE response. DPOAE amplitudes 3 h after heat stress were enhanced at f_2 = 7.4 and 9.8 kHz with statistical significance ($P < 0.05$ by two-way ANOVA), while they were slightly enhanced at f_2 = 14.1 kHz without statistical significance ($P > 0.05$ by two-way ANOVA). During the measurements, the noise floors typically ranged between –23 and –10 dB SPL and between –22 and –6 dB SPL in the control and the anesthesia + heat groups, respectively, depending on the test frequencies. DPOAE responses at every test frequency in both groups were above these noise floors when the stimulus level of f_1 was higher than 30 dB SPL.

3. Discussion

3.1. *Effects of heat stress on structure of OHCs: Young's modulus and F-actin*

To clarify how the structure of OHCs is modified due to conditioning, Young's modulus and the amount of F-actin of OHCs in the mouse cochlea were investigated in parallel before and after conditioning with heat stress. As shown in Fig. 1B, conditioning with heat stress caused an increase in Young's modulus of mouse OHCs at 3 h after heat stress, such

increase reaching a peak at 6 h. This factor returned to the pre-conditioning level by 24–48 h after heat stress. As shown in Fig. 2C, the average intensity of the F-actin labeling began to increase by 3 h after heat stress and peaked at 12 h. It then began to decrease by 24 h and returned to the pre-conditioning level by 48–96 h after heat stress. The increase and decrease in Young's modulus of OHCs showed tendencies similar to those in the amount of their F-actin. This result suggests that the increase of F-actin due to heat stress presumably led to an increase of Young's modulus of OHCs since F-actin is a primary component of the cytoskeleton of OHCs which contributes the mechanical properties of the cells (Oghalai et al., 1998; Sugawara and Wada, 2001a,b).

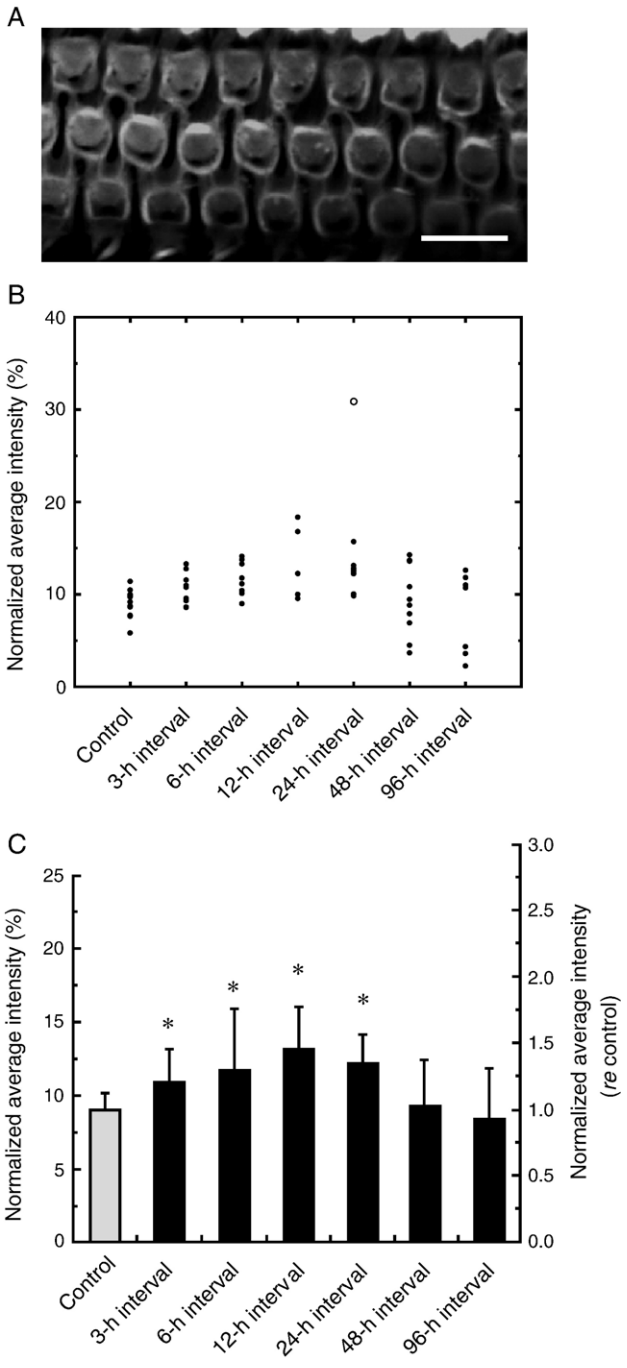

Fig. 2 – F-actin labeling at the lateral wall of the apical-turn mouse OHCs in the control group (n = 13) and the anesthesia + heat groups with 3-h (n = 10), 6-h (n = 8), 12-h (n = 6), 24-h (n = 10), 48-h (n = 10) and 96-h (n = 8) intervals. (A) The fluorescence image of F-actin labeling at the lateral wall of the OHC. Scale bar is 10 μm. (B) Normalized average intensities of F-actin labeling in each experimental group. The open circle in the anesthesia + heat group with a 24-h interval is the datum which was statistically found to be an outlier (P < 0.05 by Grubbs' test), thus being excluded from further analysis. (C) The mean and standard deviation of the normalized average intensities of F-actin labeling in each group. Average intensity of F-actin labeling increased 1.2-fold, 1.3-fold and 1.5-fold by 3 h, 6 h and 12 h after heat stress, respectively, at which point it reached a peak. It then began to decrease by 24 h and returned to the pre-conditioning level by 48–96 h. Statistical analysis indicated significant differences between the control group and the anesthesia + heat groups with intervals of 3 h, 6 h, 12 h and 24 h, as shown by asterisks (P < 0.05 by Student's t-test).

Although the exact mechanism of the increase of F-actin due to heat stress is unclear, the regulation of heat shock proteins (HSPs) is a likely candidate as a source of such increase. It has been reported that HSPs, such as HSP27 and HSP70, were expressed in the cochlea and that their expression increased in response to various kinds of stress, including heat stress (Lavoie et al., 1993, 1995; Leonova et al., 2002; Sugahara et al., 2003; Welch, 1992; Yoshida et al., 1999). Among such HSPs, HSP27 is known as a regulator of F-actin polymerization, which acts as a barbed-end F-actin capping protein and inhibits actin polymerization. Although HSP27 predominantly exists as an unphosphorylated form under normal conditions, heat stress induces rapid phosphorylation of pre-existing HSP27, promoting a loss of its actin capping activity (Clark and Muchowski, 2000). In the cochlea, the expression and localization of HSP27 have been previously confirmed at the cuticular plate and the lateral walls of OHCs (Leonova et al., 2002). Based on these reports, in the present study, the polymerization of F-actin may possibly have been accelerated by conditioning with heat stress and caused the amount of F-actin in OHCs to increase, thereby leading to an increase in Young's modulus of OHCs.

3.2. *Effects of heat stress on function of OHCs: DPOAEs*

To explore how the function of OHCs is modified due to conditioning, DPOAEs were measured before and after conditioning with heat stress. We confirmed the statistically significant enhancement of DPOAEs 3 h after heat stress at f_2 = 7.4 and 9.8 kHz and the slight enhancement without statistical significance at 14.1 kHz (Fig. 3). This result, namely, that the conditioning-induced enhancement of DPOAE levels tends to be greater at lower test frequencies, is consistent with previous findings (Kujawa and Liberman, 1999; Wang and Liberman, 2002; Yoshida and Liberman, 2000; Yoshida et al., 1999), although the exact reason for the different levels of DPOAE enhancement in different test frequencies is still

unclear. However, the enhancement of DPOAEs is probably due to functional change of OHCs since DPOAEs substantially rely on the electromotility of OHCs.

By considering a possible generation mechanism of DPOAEs using an equivalent mechanical model of the organ of Corti, a relationship between the heat stress-induced increase in the stiffness of OHCs and an enhancement of DPOAE amplitude can be explained. As previously reported, the BM is distorted toward the scala vestibuli in association with the contraction of OHCs in the cochlea, while the reticular lamina (RL), which forms a rigid structure with the pillar cells, is not distorted; rather, the rigid structure rotates around a pivot beneath the inner hair cell (Mammano and Ashmore, 1993, 1995). If we make a simplifying assumption based on these reports, the BM can be likened to a spring with a stiffness of k_{BM} and the RL can be expressed as a rigid wall since it is undeformable. Regarding the OHC, it can be represented as a series of a displacement generator (DG), i.e., the motor protein prestin, and a spring indicating the stiffness of the OHC, k_{OHC}, as previously reported (Hallworth, 1995; He and Dallos, 1999, 2000). An equivalent mechanical model of the organ of Corti was constructed by a series of those three components, as shown in Fig. 4. Based on this model, when

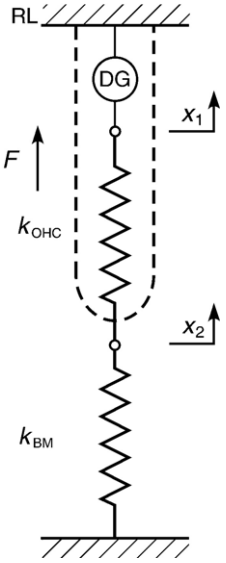

Fig. 4 – Equivalent mechanical model of the organ of Corti. The organ of Corti was expressed as a series consisting of the RL, which was expressed as a rigid wall since it is undeformable, the OHC, which was represented by a series of a displacement generator (DG), i.e., the motor protein prestin, and a spring indicating the OHC stiffness, k_{OHC}, and the BM, which was shown as a spring with a stiffness of k_{BM}. When the DG deforms x_1, the OHC subject the BM to force, F, leading to a certain amount of displacement of the BM, x_2.

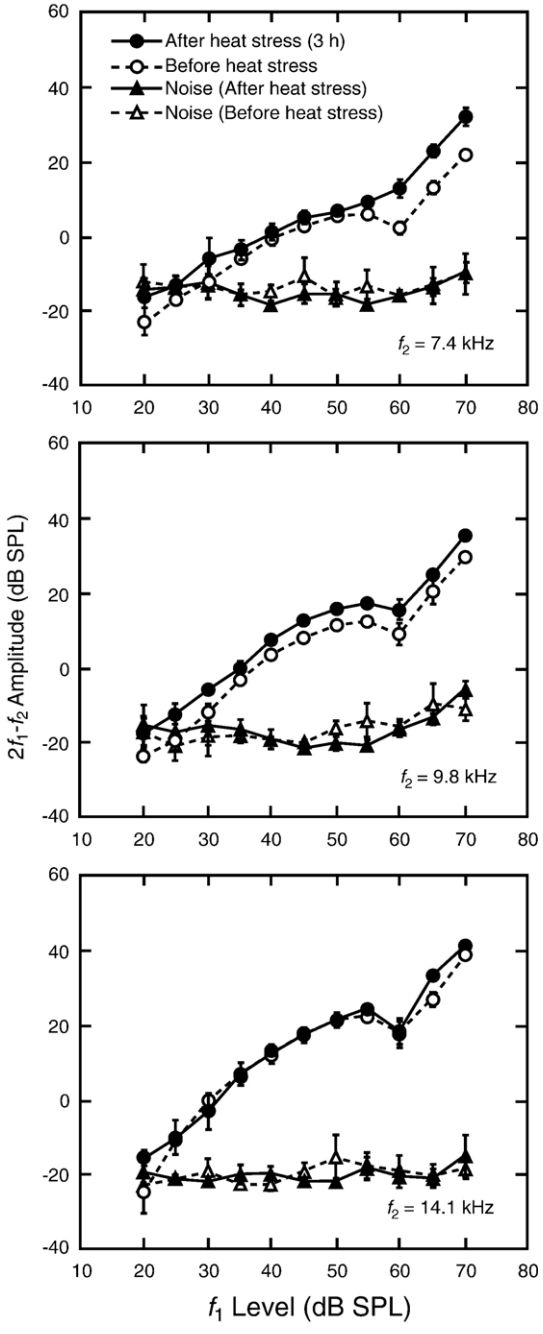

Fig. 3 – DPOAE amplitude as a function of the stimulus level of f_1. DPOAEs at $2f_1$–f_2 were measured at three frequencies (f_2 = 7.4, 9.8 and 14.1 kHz) before (n = 3) and 3 h after heat stress (n = 5). The stimulus level of f_1 was varied from 20 to 70 dB SPL with the steps of 5 dB SPL, while the stimulus level of f_2 was always 10 dB less than that of f_1; the primary frequency ratio f_2/f_1 was kept constant at 1.20. DPOAE amplitudes 3 h after heat stress at f_2 = 7.4 and 9.8 kHz were enhanced with statistical significance ($P < 0.05$ by two-way ANOVA), while they were slightly enhanced at f_2 = 14.1 kHz without statistical significance ($P > 0.05$ by two-way ANOVA). During the measurements, the noise floor typically ranged between –23 and –10 dB SPL and between –22 and –6 dB SPL in the control and the anesthesia + heat groups, respectively, depending on the test frequencies. DPOAE responses at every test frequency in both groups were above these noise floors when the stimulus level of f_1 was higher than 30 dB SPL.

the DG deforms x_1, the force generated by the OHC, F, is given by

$$F = \frac{k_{OHC}\, k_{BM}}{k_{OHC} + k_{BM}} X_1 = \frac{K_{BM}}{1 + \frac{k_{BM}}{k_{OHC}}} x_1 \quad (1)$$

According to Hooke's law, displacement of the BM, x_2, is given by

$$x_2 = \frac{F}{k_{BM}} \quad (2)$$

Assuming a cylindrical shape and homogeneity of the OHC, the stiffness of the OHC, k_{OHC}, is proportional to its Young's modulus. An increase in Young's modulus of OHCs therefore results in an increase in the stiffness of OHCs, k_{OHC}. Derived from Eq. (1), greater stiffness of OHCs, k_{OHC}, results in greater force generated by OHC, F. Consequently, the displacement of the BM, x_2, is amplified (Eq. (2)), leading to an enhancement of DPOAE amplitude.

3.3. *Mechanism of conditioning-related cochlear protection*

Yoshida et al. (1999) reported the effect of previous conditioning with whole-body heat stress on PTS. According to their report, PTS was smallest when the heat stress conditioning–trauma interval was 6 h, indicating that the largest protective effect was realized with approximately 25 dB suppression. This protective effect remained up to 12 h after the conditioning but was no longer statistically significant at 24 h and 48 h and completely disappeared by 96 h after heat stress. Interestingly, this trend is consistent with that obtained in the present study; that is, conditioning with heat stress resulted in a statistically significant increase in Young's modulus of OHCs at 3–6 h after heat stress, and such modulus then began to decrease by 12 h and returned to the pre-conditioning level at 48 h after heat stress. Since PTS is thought to be directly concerned with the mechanical damage of OHCs as described previously (Saunders et al., 1985), this congruous time course between PTS and Young's modulus of OHCs suggests that heat stress structurally modifies OHCs, resulting in an increase in their stiffness due to the increase of F-actin, and thereby OHCs possibly experience less strain when they are exposed to loud noise, resulting in protection of mammalian hearing from traumatic noise exposure.

This protective mechanism of the ear against exposure to loud noise is different from that proposed by Hu and Henderson (1997). They reported that a decrease in the cell stiffness was a factor possibly responsible for protecting the ear against exposure to loud noise. However, the conditioner of their study and that of our study are completely different. Namely, they used low-frequency octave band noise centered at 0.5 kHz at 90 dB SPL for 6 h/day, while we used 15-min whole-body heat stress. Therefore, the difference in the proposed mechanisms of cochlear protection might be due to such different conditioners.

If the conditioned ear were exposed to acoustic overstimulation, more damage to the ear would be predicted since greater BM vibration is produced by greater force of OHCs as explained in Section 3.2. However, for example, PTS is suppressed by approximately 25 dB in the heat-stressed ear (Yoshida et al., 1999), while it reaches 40 dB in the non-conditioned ear since only stereocilia are damaged (Liberman, 1987; Liberman and Dodds, 1984). This implies that the OHC stereocilia are likely stiff enough to withstand the greater mechanical stress even though heat stress increases BM motion. Morphological and histological studies of stereocilia and the lateral wall of OHCs after heat stress using AFM, electron microscopy, CLSM, etc., are needed to obtain more detailed information concerning this mechanism.

3.4. *Changes in ion concentration and protein expression in OHCs responsible for cochlear protection*

As for changes in ion concentration in OHCs, it has been reported that OHCs showed an elevation of the intracellular Ca^{2+} concentration by exposure to mechanical or acoustical stimulation, which mimicked the mechanical stress to OHCs caused by acoustical overstimulation of the ear, and that the OHC electromotility decreased with a slow shortening of cell soma and an increase in cell stiffness (Borkó et al., 2005; Fridberger et al., 1998). In these reports, those changes of OHCs were thought to produce inhibition of the cochlear output, i.e., less displacement amplitude of the BM, by which the ear was probably protected from acoustic injury. In another study, it has been reported that OHCs showed an elevation of the intracellular Ca^{2+} concentration by application of acetylcholine (ACh), which is the principle efferent neurotransmitter in the cochlea and is released by overexposure to traumatic sound (for review, see Rajan, 1992), and that OHCs showed an increase in electromotility along with a decrease in cell stiffness (Dallos et al., 1997; Sziklai et al., 2001). The influence of the medial efferent system on cochlear response is known to be inhibitory and thus provides protection against exposure to loud noise. The interaction between the increased electromotility of OHCs and the alleged inhibition of cochlear response are, however, still controversial.

Although the changes in cell stiffness and the resultant changes in electromotility of OHCs are various in the above-mentioned reports, such changes are associated with a common cause, i.e., an increase in intracellular Ca^{2+} concentration. This increase in Ca^{2+} concentration possibly results in different signaling cascades in OHCs depending on cell conditions; that is, activation of Rho kinase, which leads to an increase in cell stiffness, and/or phosphorylation of cytoskeletal proteins, which leads to a decrease in cell stiffness. Considering these reports, the response of OHCs to heat stress preconditioning that leads to functional changes could also possibly be related to the ionic responses of the cells. That is, there is a possibility that heat stress preconditioning results in an increase in intracellular Ca^{2+} concentration of OHCs and subsequent changes in electromotility of OHCs, and that such changes in electromotility influence the DPOAE response. However, since the changes in structure and function of OHCs as we herein reported as well as previously reported were due to different causes, it is difficult to compare those results. Especially, in the present study, the changes of OHCs were induced by "conditioning" with heat stress, not by ACh nor mechanical stimulation nor acoustical stimulation directly applied to OHCs in vitro. To elucidate the detailed mechanisms of ionic response responsible for cochlear

protection against exposure to loud noise, further data and analysis will be required in the future.

Regarding changes in protein expression in OHCs, it has been reported that HSP27 and HSP70 were expressed in the cochlea and that their expression increased in response to various kinds of stress, as mentioned in Section 3.1 (Lavoie et al., 1993, 1995; Leonova et al., 2002; Sugahara et al., 2003; Welch, 1992; Yoshida et al., 1999). Recently, HSP27 and HSP70 have been reported to inhibit cell apoptosis by binding cytochrome c released from the mitochondria and by binding Apaf-1, respectively. Due to those bindings, formation of apoptosome is prevented and thereby the downstream activation of the caspase cascade is inhibited, including the activation of caspase-3, resulting in the prevention of apoptosis (Green, 1998; Xanthoudakis and Nicholson, 2000). Based on these reports, although to what degree HSPs contribute to cochlear protection mechanism is unknown, the involvement of HSPs cannot be ruled out as another possible protective mechanism of the cochlea.

4. Experimental procedures

4.1. Experimental groups and design

The care and use of the animals in this study were approved by the Institutional Animal Care and Use Committee of Tohoku University, Sendai, Japan.

CBA/JNCrj strain male mice (Charles River Laboratories Japan, Kanagawa, Japan), aged 10–12 weeks (25–30 g), were divided into two groups, i.e., a control group and an anesthesia + heat group, the latter being subjected to different manipulations as shown in Fig. 5. The control group was used to establish the normal Young's modulus and amount of F-actin of OHCs and was not subjected to any stress. In the anesthesia + heat group, animals were anesthetized and heat-stressed for 3, 6, 12, 24 and 48 h before AFM measurement. For investigation of F-actin of OHCs, animals were anesthetized and heat-stressed for 3, 6, 12, 24, 48 and 96 h before CLSM measurement. Each experiment was performed by investigators blind to the groups.

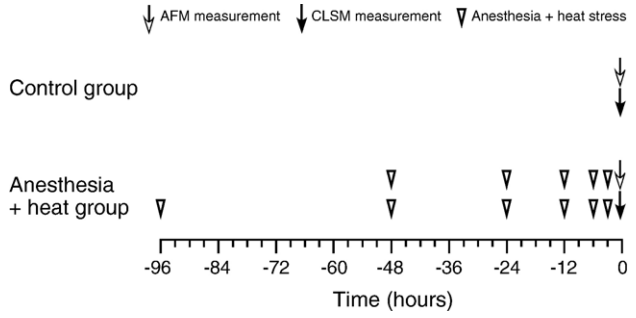

Fig. 5 – Schematic illustration of the experimental design. Animals were divided into two groups, i.e., a control group for establishing the normal properties of OHCs in the 10- to 12-week-old CBA/JNCrj mice and an anesthesia + heat group. In the anesthesia + heat group, to measure Young's modulus of OHCs, animals were anesthetized and heat-stressed (triangles) for 3, 6, 12, 24 and 48 h before AFM measurement (white arrows). For investigation of F-actin of OHCs, animals were anesthetized and heat-stressed (triangles) for 3, 6, 12, 24, 48 and 96 h before CLSM measurement (black arrows).

4.2. Heat stress

Animals were heat-stressed as described previously (Yoshida et al., 1999). The rectal temperatures of the animals were monitored using a rectal thermometer while application of anesthesia and heat stress. First, the animals were anesthetized with ketamine (60 mg/kg, i.p.) and xylazine (6 mg/kg, i.p.). After the injection, the animals were then immediately placed on a heating pad maintained at 37 °C to prevent hypothermia during the anesthesia. The rectal temperature stayed at 36.5 °C (±0.5 °C) during the anesthetization procedure. Once the animals were deeply anesthetized (approximately 10 min after injection), they were placed in an aluminum boat floating in a hot water bath maintained at 46.5 °C. To avoid direct effects of heat from the bottom of the boat to the animal, the animal's head was placed on a gaze pad. The rectal temperature was controlled by putting the aluminum boat in and taking it out of the hot water bath. The rectal temperature was raised at an average rate of 0.6 °C/min. After it reached 41.5 °C, it was maintained at that temperature for 15 min. The animals were then transferred from the boat to the heating pad to fully recover from the anesthesia before being returned to the animal care facility.

4.3. Cell preparation

Just before the AFM/CLSM measurement, the animals were decapitated and the cochleae were detached from the animals in tissue culture medium (Leibovitz's L-15, Invitrogen, Carlsbad, CA). To measure OHC Young's modulus, OHCs were isolated as previously described (Murakoshi et al., 2006). The cochleae were dissected out from the bullae and transferred into fresh L-15 medium. The bony shell covering the cochlea was then removed from the oval window toward the apex by an angled pick with a sharpened tip. The BM and the organ of Corti were simultaneously detached from the basal end of the modiolus toward its apical end with forceps. The dissected coiled tissue was then severed into two pieces, i.e., the apical turn and the basal turn. Only the apical turn was used in this study, since the cells of the organ of Corti in the basal turn are vulnerable and thus are destroyed during dissection. The tissue was then digested in 1 ml of L-15 medium containing 1 mg of type IV collagenase (Sigma-Aldrich, St. Louis, MO) for 15 min. After the incubation, the tissue was transferred into enzyme-free L-15 medium in a glass-bottomed dish, the glass surface of which was coated with poly-D-lysine (MatTek, Ashland, MA). Solitary OHCs were isolated by gently triturating the coiled tissue in that medium with a 200-μl pipette (Gilson, Villiers, France). They were then left at rest for a few minutes to become attached to the bottom of the dish. For the subsequent AFM measurement, cells showing no obvious signs of deterioration such as shrinkage, swelling and/or translocation of the nucleus were selected and the measurement was carried out within 1 h after the isolation of OHCs from the organ of Corti.

For investigation of F-actin of OHCs, tissue in the cochlea was fixed by perfusion with 4% paraformaldehyde via the

round window and subsequent immersion of the cochlea in the same fixative for 1 h. The coiled tissue was then removed as described above and kept in the same fixative for 30 min. The coiled tissue was permeabilized with 0.5% Triton X-100 (ICN Biomedicals, Aurora, OH) for 30 min. After incubation with Block Ace (Dainippon Pharmaceutical, Osaka, Japan) for 30 min, the tissue was then stained with 0.3 μM rhodamine–phalloidin (Sigma-Aldrich, St. Louis, MO) for 3 h. All experiments were performed at room temperature.

4.4. *Atomic force microscopy*

An AFM (NVB100, Olympus, Tokyo, Japan) equipped with a V-shaped silicon nitride cantilever (OMCL-TR400PSA-2, Olympus, Tokyo, Japan) with a spring constant of 0.08 N/m was used for the experiments. To measure Young's modulus of the mouse OHCs, an indentation test using the AFM was carried out as described elsewhere (Murakoshi et al., 2006). When the cantilever is moved by the piezoelectric scanner and the tip of the cantilever comes in contact with the sample, the cantilever starts to deflect, the deflection of the cantilever being optically detected by a laser system. By this measurement, the relationship between the cantilever deflection d and the sample indentation δ is obtained. The curve of this relationship is fitted with the following square regression line:

$$d = a\delta^2 \tag{3}$$

where a is the slope of this curve, which represents the elastic properties of the sample.

When subjects are elastic, isotropic, homogeneous and semi-infinite and when the indentation tip is rigid and conical, the Hertz model, which describes the elastic response of material indented by the tip, can be applied to the measurement data. According to the Hertz model, the relationship between the cantilever deflection d and the indentation δ is defined as follows:

$$d = \{2E\ \tan\alpha/\pi k(1-\upsilon^2)\}\delta^2 \tag{4}$$

where E, α, k and υ are Young's modulus of the sample, the half-opening angle of the cantilever, the spring constant of the cantilever and Poisson's ratio of the sample, respectively (Sneddon, 1965; Wu et al., 1998). In this study, the half-opening angle and the spring constant of the cantilever were 17° and 0.08 N/m, respectively. Poisson's ratio was assumed to be 0.499 because the samples were incompressible biomaterials. Since the slope a in Eq. (3) corresponds to $2E\tan\alpha/\pi k(1-\upsilon^2)$ in Eq. (4), Young's modulus of the sample, E, can be obtained. To reduce the variance of Young's modulus and due to the limited time available for measurement in this experiment, all measurements were conducted in the central part of the middle region of the OHC and the mean value of four Young's moduli measured at that point were defined as Young's modulus of the OHC (Murakoshi et al., 2006).

4.5. *Confocal laser scanning microscopy*

A CLSM (FV500, Olympus, Tokyo, Japan) equipped with a UPlan Apo 60 × (NA = 1.40) oil-immersion objective and a helium neon laser (543 nm) was used for the experiments. To investigate the amount of F-actin, fluorescence images of F-actin at the lateral wall of OHCs (3 μm below the cuticular plate), which were stained with rhodamine–phalloidin, were obtained from the dissected apical turn of the organ of Corti. The total intensity of each pixel within a circle with a diameter of 8 μm, in which an OHC was located, was defined as the intensity of one OHC. For intensity analysis, the morphology of OHCs was microscopically examined, and intensities of 16 OHCs with no obvious deterioration were obtained and averaged. In the obtained images, each pixel has an intensity value ranging from 0 (dark) to 4,095 (light), i.e., 12 bits per pixel. The average intensity was normalized by the total value of the maximum intensities of the pixels located in the 16 circles ($4095 \times$ number of pixels located in the 16 circles $= 1.8 \times 10^6$), which was termed "normalized average intensity." Since the fluorescent intensity is proportional to the amount of fluorescent substance specifically conjugated with the target when the preparation and the observation are performed under the same condition, the obtained intensity of F-actin labeling is proportional to the amount of F-actin.

4.6. *Testing of DPOAEs*

Animals were anesthetized with ketamine (60 mg/kg, i.p.) and xylazine (6 mg/kg, i.p.). After the injection, the animals were placed on a heating pad maintained at 37 °C to prevent hypothermia during the anesthesia. DPOAEs were measured using an ER-10C (Etymotic Research, Elk Grove Village, IL) acoustic system having two speakers and one microphone. A custom-made probe tip fitted to the mouse external auditory canal was used in this study. DPOAEs (at a frequency of $2f_1$–f_2) were evoked by two pure tones (at frequencies of f_1 and f_2). The primary frequency ratio f_2/f_1 was kept constant at 1.20. The stimulus level of f_1 was varied from 20 to 70 dB SPL with steps of 5 dB SPL, while the stimulus level of f_2 was always 10 dB less than that of f_1. DPOAEs were measured at three frequencies, i.e., f_2 = 7.4, 9.8 and 14.1 kHz. According to the place-frequency map reported by Müller et al. (2005), the audible frequency range of mice is from 4.8 kHz to 79.1 kHz. In the present study, therefore, we chose 7.4 kHz as the lowest test frequency of f_2. Since the primary frequency ratio f_2/f_1 was kept constant at 1.20, the test frequency of f_1 was 6.2 kHz, which was close to the lowest audible frequency 4.8 kHz. The highest test frequency of f_2 was set at 14.1 kHz because the speaker in the acoustic system used in this study, ER-10C, could not generate required sound pressure for the DPOAE measurement above around 15.0 kHz. The two primaries were presented for 4.096 s. The resulting output from the ear canal was sampled (sampling rate, 20.48 ms; number of data, 1024) and averaged for 200 times. The amplitude of the $2f_1$–f_2 distortion product was then computed by fast Fourier transformation (FFT).

Acknowledgments

The authors are grateful to M. Charles Liberman, PhD, and David Z. Z. He, PhD, for helpful suggestions and comments on the manuscript.

This work was supported by Grant-in-Aid for Scientific Research on Priority Areas 15086202 from the Ministry of Education, Culture, Sports, Science and Technology of Japan, by a Health and Labour Science Research Grant from the Ministry of Health, Labour and Welfare of Japan, by a grant from the Human Frontier Science Program to H.W., by Special Research Grant 11170012 from the Tohoku University 21st Century COE Program of the "Future Medical Engineering Based on Bio-nanotechnology" to M.M. and by Grant-in-Aid for Scientific Research 17591774 from the Ministry of Education, Culture, Sports, Science and Technology of Japan to N.Y.

REFERENCES

Ashmore, J.F., 1987. A fast motile response in guinea-pig outer hair cells: the cellular basis of the cochlear amplifier. J. Physiol. 388, 323–347.

Avinash, G.B., Nuttall, A.L., Raphael, Y., 1993. 3-D analysis of F-actin in stereocilia of cochlear hair cells after loud noise exposure. Hear. Res. 67, 139–146.

Borkó, R., Batta, T.J., Sziklai, I., 2005. Slow motility, electromotility and lateral wall stiffness in the isolated outer hair cells. Hear. Res. 207, 68–75.

Brownell, W.E., Bader, C.R., Bertrand, D., de Ribaupierre, Y., 1985. Evoked mechanical responses of isolated cochlear outer hair cells. Science 227, 194–196.

Campo, P., Subramaniam, M., Henderson, D., 1991. The effect of 'conditioning' exposures on hearing loss from traumatic exposure. Hear. Res. 55, 195–200.

Canlon, B., Borg, E., Flock, A., 1988. Protection against noise trauma by pre-exposure to a low level acoustic stimulus. Hear. Res. 34, 197–200.

Canlon, B., Lofstrand, P., Borg, E., 1993. Ultrastructural changes in the presynaptic region of outer hair cells after acoustic stimulation. Neurosci. Lett. 150, 103–106.

Clark, J.I., Muchowski, P.J., 2000. Small heat-shock proteins and their potential role in human disease. Curr. Opin. Struct. Biol. 10, 52–59.

Dallos, P., He, D.Z., Lin, X., Sziklai, I., Mehta, S., Evans, B.N., 1997. Acetylcholine, outer hair cell electromotility, and the cochlear amplifier. J. Neurosci. 17, 2212–2226.

Franklin, D.J., Lonsbury-Martin, B.L., Stagner, B.B., Martin, G.K., 1991. Altered susceptibility of 2f1-f2 acoustic-distortion products to the effects of repeated noise exposure in rabbits. Hear. Res. 53, 185–208.

Fridberger, A., Flock, A., Ulfendahl, M., Flock, B., 1998. Acoustic overstimulation increases outer hair cell Ca2+ concentrations and causes dynamic contractions of the hearing organ. Proc. Natl. Acad. Sci. U. S. A. 95, 7127–7132.

Green, D.R., 1998. Apoptotic pathways: the roads to ruin. Cell 94, 695–698.

Hallworth, R., 1995. Passive compliance and active force generation in the guinea pig outer hair cell. J. Neurophysiol. 74, 2319–2328.

He, D.Z., Dallos, P., 1999. Somatic stiffness of cochlear outer hair cells is voltage-dependent. Proc. Natl. Acad. Sci. U. S. A. 96, 8223–8228.

He, D.Z., Dallos, P., 2000. Properties of voltage-dependent somatic stiffness of cochlear outer hair cells. J. Assoc. Res. Otolaryngol. 1, 64–81.

Hu, B.H., Henderson, D., 1997. Changes in F-actin labeling in the outer hair cell and the Deiters cell in the chinchilla cochlea following noise exposure. Hear. Res. 110, 209–218.

Kachar, B., Brownell, W.E., Altschuler, R., Fex, J., 1986. Electrokinetic shape changes of cochlear outer hair cells. Nature 322, 365–368.

Kujawa, S.G., Liberman, M.C., 1997. Conditioning-related protection from acoustic injury: effects of chronic deafferentation and sham surgery. J. Neurophysiol. 78, 3095–3106.

Kujawa, S.G., Liberman, M.C., 1999. Long-term sound conditioning enhances cochlear sensitivity. J. Neurophysiol. 82, 863–873.

Lavoie, J.N., Hickey, E., Weber, L.A., Landry, J., 1993. Modulation of actin microfilament dynamics and fluid phase pinocytosis by phosphorylation of heat shock protein 27. J. Biol. Chem. 268, 24210–24214.

Lavoie, J.N., Lambert, H., Hickey, E., Weber, L.A., Landry, J., 1995. Modulation of cellular thermoresistance and actin filament stability accompanies phosphorylation-induced changes in the oligomeric structure of heat shock protein 27. Mol. Cell. Biol. 15, 505–516.

Leonova, E.V., Fairfield, D.A., Lomax, M.I., Altschuler, R.A., 2002. Constitutive expression of Hsp27 in the rat cochlea. Hear. Res. 163, 61–70.

Liberman, M.C., 1987. Chronic ultrastructural changes in acoustic trauma: serial-section reconstruction of stereocilia and cuticular plates. Hear. Res. 26, 65–88.

Liberman, M.C., Dodds, L.W., 1984. Single-neuron labeling and chronic cochlear pathology: III. Stereocilia damage and alterations of threshold tuning curves. Hear. Res. 16, 55–74.

Mammano, F., Ashmore, J.F., 1993. Reverse transduction measured in the isolated cochlea by laser Michelson interferometry. Nature 365, 838–841.

Mammano, F., Ashmore, J.F., 1995. A laser interferometer for sub-nanometre measurements in the cochlea. J. Neurosci. Methods 60, 89–94.

Miller, J.D., 1974. Effects of noise on people. J. Acoust. Soc. Am. 56, 729–764.

Miller, J.D., Watson, C.S., Covell, W.P., 1963. Deafening effects of noise on the cat. Acta Oto-laryngol. Suppl. (Stockh.) 176, 1–89.

Miyakita, T., Hellstrom, P.A., Frimanson, E., Axelsson, A., 1992. Effect of low level acoustic stimulation on temporary threshold shift in young humans. Hear. Res. 60, 149–155.

Müller, M., von Hünerbein, K., Hoidis, S., Smolders, J.W.T., 2005. A physiological place-frequency map of the cochlea in the CBA/J mouse. Hear. Res. 202, 63–73.

Murakoshi, M., Yoshida, N., Iida, K., Kumano, S., Kobayashi, T., Wada, H., 2006. Local mechanical properties of mouse outer hair cells: atomic force microscopic study. Auris, Nasus, Larynx. 33, 149–157.

Oghalai, J.S., Patel, A.A., Nakagawa, T., Brownell, W.E., 1998. Fluorescence-imaged microdeformation of the outer hair cell lateral wall. J. Neurosci. 18, 48–58.

Pukkila, M., Zhai, S., Virkkala, J., Pirvola, U., Ylikoski, J., 1997. The "toughening" phenomenon in rat's auditory organ. Acta Oto-laryngol., Suppl. 529, 59–62.

Rajan, R., 1992. Protective functions of the efferent pathways to the mammalian cochlea. Mosby-Year Book Inc., St. Louise.

Ryan, A.F., Bennett, T.M., Woolf, N.K., Axelsson, A., 1994. Protection from noise-induced hearing loss by prior exposure to a nontraumatic stimulus: role of the middle ear muscles. Hear. Res. 72, 23–28.

Santos-Sacchi, J., Dilger, J.P., 1988. Whole cell currents and mechanical responses of isolated outer hair cells. Hear. Res. 35, 143–150.

Saunders, J.C., Dear, S.P., Schneider, M.E., 1985. The anatomical consequences of acoustic injury: a review and tutorial J. Acoust. Soc. Am. 78, 833–860.

Skellett, R.A., Cullen Jr., J.K., Fallon, M., Bobbin, R.P., 1998. Conditioning the auditory system with continuous vs. interrupted noise of equal acoustic energy: is either exposure more protective? Hear. Res. 116, 21–32.

Sneddon, I.N., 1965. The relation between load and penetration in

the axisymmetric Boussinesq problem for a punch of arbitrary profile. Int. J. Eng. Sci. 3, 47–57.
Sugahara, K., Inouye, S., Izu, H., Katoh, Y., Katsuki, K., Takemoto, T., Shimogori, H., Yamashita, H., Nakai, A., 2003. Heat shock transcription factor HSF1 is required for survival of sensory hair cells against acoustic overexposure. Hear. Res. 182, 88–96.
Sugawara, M., Wada, H., 2001a. Analysis of elastic properties of outer hair cell wall using shell theory. Hear. Res. 160, 63–72.
Sugawara, M., Wada, H., 2001b. Analysis of force production of the auditory sensory cell. In: Cheng, L., et al. (Ed.), The 8th International Congress on Sound and Vibration, Hong Kong, pp. 917–924.
Sziklai, I., Szonyi, M., Dallos, P., 2001. Phosphorylation mediates the influence of acetylcholine upon outer hair cell electromotility. Acta Oto-laryngol. 121, 153–156.
Wang, Y., Liberman, M.C., 2002. Restraint stress and protection from acoustic injury in mice. Hear. Res. 165, 96–102.
Welch, W.J., 1992. Mammalian stress response: cell physiology, structure/function of stress proteins, and implications for medicine and disease. Physiol. Rev. 72, 1063–1081.
Wu, H.W., Kuhn, T., Moy, V.T., 1998. Mechanical properties of L929 cells measured by atomic force microscopy: effects of anticytoskeletal drugs and membrane crosslinking. Scanning 20, 389–397.
Xanthoudakis, S., Nicholson, D.W., 2000. Heat-shock proteins as death determinants. Nat. Cell Biol. 2, E163–E165.
Yoshida, N., Liberman, M.C., 2000. Sound conditioning reduces noise-induced permanent threshold shift in mice. Hear. Res. 148, 213–219.
Yoshida, N., Kristiansen, A., Liberman, M.C., 1999. Heat stress and protection from permanent acoustic injury in mice. J. Neurosci. 19, 10116–10124.